(KTeV collaboration), *Phys. Rev. Lett.* **83**, 2128 (1999).
59. See S. D. Wick, T. W. Kephart, T. J. Weiler, P. L. Biermann, http://xxx.lanl.gov/abs/astro-ph/0001233.
60. S. Bonazzola, P. Peter, *Astropart. Phys.* **7**, 161 (1997).
61. G. R. Farrar, P. L. Biermann, *Phys. Rev. Lett.* **81**, 3579 (1998); C. M. Hoffman, *Phys. Rev. Lett.* **83**, 2471 (1999); G. R. Farrar, P. L. Biermann, *Phys. Rev. Lett.* **83**, 2472 (1999); G. Sigl, D. F. Torres, L. A. Anchordoqui, G. E. Romero, http://xxx.lanl.gov/abs/astro-ph/0008363; A. Virmani *et al.*, http://xxx.lanl.gov/abs/astro-ph/0010235.
62. The technical term in quantum field theory is "unitarity."
63. H. Goldberg, T. J. Weiler, *Phys. Rev. D* **59**, 113005 (1999).
64. G. Domokos, S. Kovesi-Domokos, *Phys. Rev. Lett.* **82**, 1366 (1999).
65. See, e.g., N. Arkani-Hamed, S. Dimopoulos, G. Dvali, *Phys. Rev. D* **59**, 086004 (1999).
66. S. Nussinov, R. Shrock, *Phys. Rev. D* **59**, 105002 (1999); P. Jain, D. W. McKay, S. Panda, J. P. Ralston, *Phys. Lett.* **B484**, 267 (2000); J. P. Ralston, P. Jain, D. W. McKay, S. Panda, http://xxx.lanl.gov/abs/hep-ph/0008153.
67. See, e.g., S. Cullen, M. Perelstein, M. E. Peskin, *Phys. Rev.D* **62**, 055012 (2000).
68. S. Cullen, M. Perelstein, *Phys. Rev. Lett.* **83**, 268 (1999); V. Barger, T. Han, C. Kao, R.-J. Zhang, *Phys. Lett. B* **461**, 34 (1999).
69. To give rise to the EASs so far observed, however, cross sections of at least a few 10^{-26} cm^2 are necessary; see M. Kachelrieß, M. Plümacher, *Phys. Rev. D* **62**, 103006 (2000); L. Anchordoqui *et al.*, http://xxx.lanl.gov/abs/hep-ph/0011097.
70. C. Tyler, A. V. Olinto, G. Sigl, http://xxx.lanl.gov/abs/hep-ph/0002257 (*Phys. Rev. D.*, in press).
71. See, e.g., S. Coleman, S. L. Glashow, *Nucl. Phys.* **B574**, 130 (2000); L. Gonzalez-Mestres, *Nucl. Phys. B* (*Proc. Suppl.*) **48**, 131 (1996).
72. See, e.g., R. Aloisio, P. Blasi, P. L. Ghia, A. F. Grillo, *Phys. Rev. D* **62**, 053010 (2000).
73. W. Rhode *et al.*, *Astropart. Phys.* **4**, 217 (1996).
74. R. M. Baltrusaitis *et al.*, *Astrophys. J.* **281**, L9 (1984); *Phys. Rev. D* **31**, 2192 (1985).
75. P. W. Gorham, K. M. Liewer, C. J. Naudet, http://xxx.lanl.gov/abs/astro-ph/9906504.
76. For general information see http://amanda.berkeley.edu/; see also F. Halzen, *New Astron. Rev.* **42**, 289 (1999).
77. For general information see http://www.ps.uci.edu/icecube/workshop.html; see also F. Halzen, *Am. Astron. Soc. Meet.* **192**, 62 28 (1998); AMANDA collaboration, talk presented at the 8th International Workshop on Neutrino Telescopes, Venice, February 1999, http://xxx.lanl.gov/abs/astro-ph/9906205.
78. R. J. Protheroe, P. A. Johnson, *Astropart. Phys.* **4**, 253 (1996); [erratum] *Astropart. Phys.* **5**, 215 (1996).
79. I acknowledge P. Biermann, P. Blasi, M. Boratav, T. Ensslin, P. Peter, R. Plaga, G. Raffelt, and A. Watson for helpful comments on the manuscript.

REVIEW

Gamma-Ray Bursts: Accumulating Afterglow Implications, Progenitor Clues, and Prospects

P. Mészáros

Gamma-ray bursts (GRBs) are sudden, intense flashes of gamma rays that, for a few blinding seconds, light up in an otherwise fairly dark gamma-ray sky. They are detected at the rate of about once a day, and while they are on, they outshine every other gamma-ray source in the sky, including the sun. Major advances have been made in the last 3 or 4 years, including the discovery of slowly fading x-ray, optical, and radio afterglows of GRBs, the identification of host galaxies at cosmological distances, and evidence showing that many GRBs are associated with star-forming regions and possibly supernovae. Progress has been made in understanding how the GRB and afterglow radiation arises in terms of a relativistic fireball shock model. These advances have opened new vistas and questions on the nature of the central engine, the identity of their progenitors, the effects of the environment, and their possible gravitational wave, cosmic ray, and neutrino luminosity. The debates on these issues indicate that GRBs remain among the most mysterious puzzles in astrophysics.

Until a few years ago, GRBs were known predominantly as bursts of γ-rays, largely devoid of any observable traces at any other wavelengths. However, a striking development in the last several years has been the measurement and localization of fading x-ray signals from some GRBs, lasting typically for days and making possible the optical and radio detection of afterglows, which, as fading beacons, mark the location of the fiery and brief GRB event. These afterglows in turn enabled the measurement of redshift distances, the identification of host galaxies, and the confirmation that GRBs were, as suspected, at cosmological distances on the order of billions of light years, similar to those of the most distant galaxies and quasars. Even at those distances, they appear so bright that their energy output must be on the order of 10^{51} to 10^{54} erg s^{-1}, larger than that of any other type of source. It is comparable to burning up the entire mass-energy of the sun in a few tens of seconds, or to emit over that same period of time as much energy as our entire Milky Way does in a hundred years.

GRBs were first reported in 1973 on the basis of 1969–1971 observations by the Vela military satellites monitoring for nuclear explosions in verification of the Nuclear Test Ban Treaty. When these mysterious γ-ray flashes, which did not come from Earth's direction, were initially detected, the first suspicion (quickly abandoned) was that they might be the product of an advanced extraterrestrial civilization. Soon, however, it was realized that this was a new and extremely puzzling cosmic phenomenon. For the next 20 years, hundreds of GRB detections were made, and frustratingly, they continued to vanish too soon to get an accurate angular position to permit any follow-up observations. The reason for this is that γ-rays are notoriously hard to focus, so γ-ray images are generally not very sharp.

The next major advance occurred in 1991 with the launch of the Compton Gamma-Ray Observatory (CGRO), whose results have been summarized in (*1*). The all-sky survey from the Burst and Transient Experiment (BATSE) onboard CGRO, which measured about 3000 bursts, showed that they were isotropically distributed, suggesting a cosmological distribution with no dipole and quadrupole components. The spectra were nonthermal, the number of photons per unit photon energy varying typically as $N(\varepsilon) \propto \varepsilon^{-\alpha}$, where $\alpha \sim 1$ at low energies changes to $\alpha \sim 2$ to 3 above a photon energy $\varepsilon_0 \sim 0.1$ to 1 MeV (*2*), the spectral power law dependence extending sometimes to GeV energies (*3*). The durations (at MeV energies) range from 10^{-3} s to about 10^3 s, with a roughly bimodal distribution of long bursts (duration $t_b \gtrsim 2$ s) and short bursts ($t_b \lesssim 2$ s) (*4*), and substructure sometimes down to milliseconds. The γ-ray light curves range from smooth, fast-rise and quasi-exponential decay, through curves with several peaks, to variable curves with many peaks (Fig. 1). The pulse distribution is complex, and the time histories of the emission as a function of energy can provide clues for the geometry of the emitting regions (*5*).

A watershed event occurred in 1997, when the Italian-Dutch satellite BeppoSAX succeeded in obtaining high-resolution x-ray images (*6*) of the predicted fading afterglow of GRB970228, followed by a number of other detections at an approximate rate of 10 per year (Fig. 2). These detections, after a 4- to 6-hour delay for processing, led to positions accurate to about an arc minute, which allowed the detection and follow-up of the afterglows at optical and longer wavelengths [e.g., (*7*)]. This paved

Department of Astronomy and Astrophysics, Pennsylvania State University, University Park, PA 16803, USA, and Institute for Theoretical Physics, University of California, Santa Barbara, CA 93106, USA. E-mail: pmeszaros@astro.psu.edu

the way for the measurement of redshift distances, the identification of candidate host galaxies, and the confirmation that they were at cosmological distances (*8, 9*). More than 30 GRB afterglows have been located, with detections sometimes extending to radio (*10*) and over time scales of many months, of which at least 25 resulted in the identification of host galaxies [e.g., (*11*)].

The Fireball Shock and Afterglow Scenario

At cosmological distances, the observed GRB fluxes imply energies on the order of up to 1 solar rest-mass ($\lesssim 10^{54}$ erg), and from causality these must arise in regions whose size is on the order of kilometers in a time scale on the order of seconds. This implies that an electron-positron and γ-ray ($e^{\pm}$, γ) fireball must form (*12–14*), which would expand relativistically. The difficulty with this was that a smoothly expanding fireball would convert most of its energy into kinetic energy of accelerated baryons rather than into luminosity, and would produce a quasi-thermal spectrum, whereas the typical time scales would not explain events much longer than milliseconds. This problem was solved with the introduction of the fireball shock model (*15, 16*). The basis of this model was that shock waves would inevitably occur in the outflow, after the fireball became transparent, and these would reconvert the kinetic energy of expansion into nonthermal particle and radiation energy. The complicated light curves can be understood in terms of internal shocks (*17*) in the outflow itself, caused by velocity variations in the outflow [compare (*18*)]. This is followed by the development of a forward shock or blast wave moving into the external medium ahead of the ejecta, and a reverse shock wave moving back into the ejecta as the latter is decelerated by the back-reaction from the external medium (Fig. 3).

Similar to what is observed by spacecraft in interplanetary shocks, the shocks in the fireball outflow are expected to be collisionless (i.e., mediated by chaotic electric and magnetic fields). The minimum random Lorentz factor of protons going through the shocks is expected to be comparable to the bulk Lorentz factor of the flow, whereas that of the electrons may exceed this by a factor of up to the ratio of the proton to the electron mass. The energy of the particles can be further boosted by diffusive shock acceleration (*19*) as they scatter repeatedly across the shock interface, acquiring a power law distribution $N(\gamma) \propto \gamma^{-p}$, where $p \sim 2$ to 3. In the presence of turbulent magnetic fields built up behind the shocks, the electrons produce a synchrotron power-law radiation spectrum (*16, 17*) similar to that observed (*2*), whereas the inverse Compton scattering of these synchrotron photons extends the spectrum into the GeV range (*20*).

The external shock becomes important when the inertia of the swept-up external matter starts to produce an appreciable slowing down of the ejecta. As the fireball continues to plow ahead, it sweeps up an increasing amount of external matter, made up of interstellar gas plus possibly gas that was previously ejected by the progenitor star. For an approximately smooth distribution of external matter, the bulk Lorentz factor of the fireball thereafter decreases as an inverse power of the time (which asymptotically is $t^{-3/8}$). As a consequence, the accelerated electron minimum random Lorentz factor and the turbulent magnetic field also decrease as inverse power laws in time. This implies that the spectrum softens in time as the synchrotron peak corresponding to the minimum Lorentz factor and field decreases (*15*), leading to the possibility of late radio (*21*) and optical emission (*22*). The GRB radiation, which started out concentrated in the γ-ray range during the burst, is expected to progressively evolve into an afterglow radiation that peaks in the x-rays, then ultraviolet (UV), optical, infrared, and radio (*23*). Detailed predictions of the afterglow properties (*23*), made in advance of the observations, agreed well with subsequent detections at these wavelengths, followed up over periods of months (Figs. 4 and 5). At a given observer frequency, after the synchrotron peak has passed through it, the observed photon flux also decreases as an inverse power law in time, typically $t^{-1.2}$ or steeper. The study of GRBs and afterglows (*24–30*) has provided confirmation of this generic fireball shock model of GRBs, in agreement with the data as recently summarized in a review (*31*). An important check on the model came from the detection of diffractive scintillation in the radio afterglow of GRB970508, which provided a direct determination of the source size and a direct confirmation of relativistic source expansion (*32, 33*).

One issue raised by the large redshifts (*9*) is that the measured γ-ray fluences imply a total photon energy on the order of 10^{52} to 10^{54} ($\Omega_\gamma/4\pi$) erg, where Ω_γ is the solid angle into which the γ-rays are beamed. For a solar-mass object, this implies that an unusually large fraction of the energy is converted into γ-ray photon energy. A beamed jet would alleviate the energy requirements, and some observational evidence suggests the

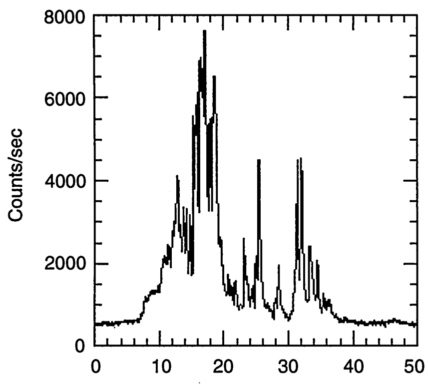

Fig. 1. Time profile of a typical GRB. The *y* axis is the photon count rate in the 0.05 to 0.5 MeV range; the *x* axis is the time in seconds since the burst trigger. Both before and after the burst trigger, no γ-rays are detectable from the same direction (*1*).

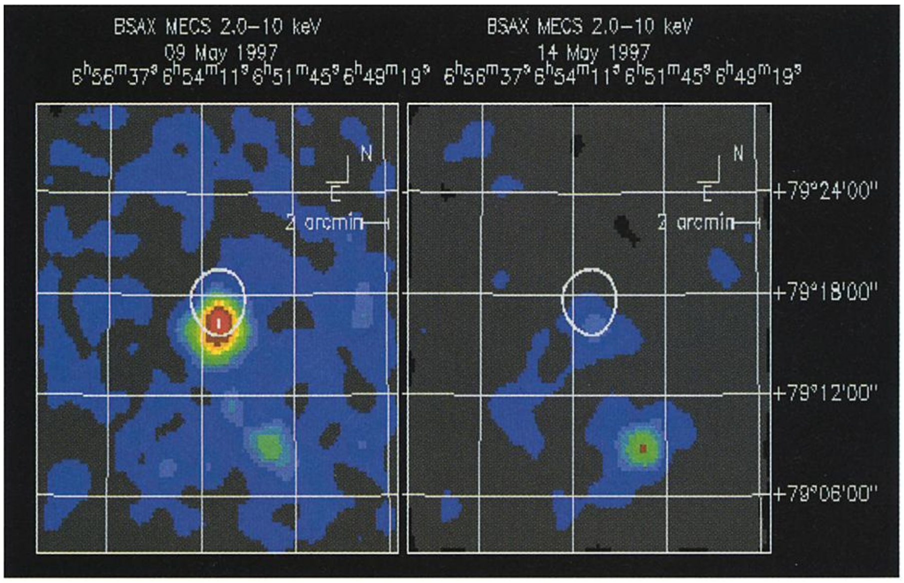

Fig. 2. BeppoSAX Narrow Field Imager pictures of the afterglow of GRB970508 in 2- to 10-keV x-rays, taken 6 hours and 3 days after the burst trigger, respectively, showing the fading intensity. The white circle is the initial Wide Field Camera error box. [Image courtesy of L. Piro and BeppoSAX GRB team]

presence of a jet (*34–37*). Whether or not a jet is present, such energies are in principle achievable for bursts arising from stellar progenitors, but a poorly understood issue is how this energy is converted into an ultrarelativistic, and possibly collimated, bulk outflow.

An observation that attracted much attention was the discovery (*38*) of a prompt and extremely bright (visual magnitude m_v $\sim$ 9) optical flash in GRB990123, 15 s after the GRB started (and while it was still going on). This is generally interpreted (*23, 39*) as the radiation from the reverse component of the external shock. However, such bright prompt flashes may be rare because they have not yet been detected from other bursts. Two other noteworthy developments are the possibility of a relation between the differential time lags for the arrival of burst pulses at different energies and the luminosity (*40*), and between the degree of variability or spikiness of the γ-ray light curve variability and the luminosity (*41, 42*). These hypotheses are based on data for bursts where an optical redshift allows a determination of the luminosity, under the assumption of isotropy. These correlations are still tentative, but if confirmed they could be used to derive independent estimates of the redshift of a GRB.

Progenitors and Environment

The progenitors of GRBs are not yet well identified. The current view of most researchers is that GRBs arise in a very small fraction ($\sim 10^{-6}$) of stars that undergo a catastrophic energy release event toward the end of their evolution. One class of candidates involves massive stars whose core collapses (*43–45*), probably in the course of merging with a companion; these are often referred to as hypernovae or collapsars (*46*). Another class of candidates consists of neutron star (NS) binaries or neutron star–black hole (BH) binaries (*12, 13, 47, 48*), which lose orbital angular momentum by gravitational wave radiation and undergo a merger. Both of these progenitor types are expected to lead to the formation of a black hole whose mass is several times that of the sun ($M_\odot$), surrounded by a temporary debris torus whose accretion can provide a sudden release of gravitational energy, with similar total energies (*49*), sufficient to power a burst. An $e^{\pm}$, γ fireball arises from the enormous compressional heating and dissipation associated with the accretion, possibly involving a small fraction of baryons and magnetic fields in excess of 10^{15} G, which can provide the driving stresses leading to the relativistic expansion. This fireball may be substantially collimated if the progenitor is a massive star, where an extended, fast-rotating envelope can provide a natural escape route or funnel for the fireball along the rotation axis (Fig. 3). Other possible alternatives include the formation from a stellar collapse of a fast-rotating neutron star with an ultrahigh magnetic field (*50–52*) or the tidal disruption of compact stars by 10^5 to 10^6 $M_\odot$ black holes (*53*).

Observations related to the possible progenitors are restricted, so far, to the class of long bursts (of γ-ray durations $t_b \sim 10$ to 10^3 s), because BeppoSAX is mainly sensitive to bursts longer than about 5 to 10 s. For these long bursts, the fading x-ray and optical afterglow emission is predominantly localized within the optical image of the host galaxy. In most cases it is offset from the center, but in a few cases (out of a total of about 20) it is near the center of the galaxy (*11*). This is in disagreement with current simple calculations of NS-NS mergers, which suggest that high spatial

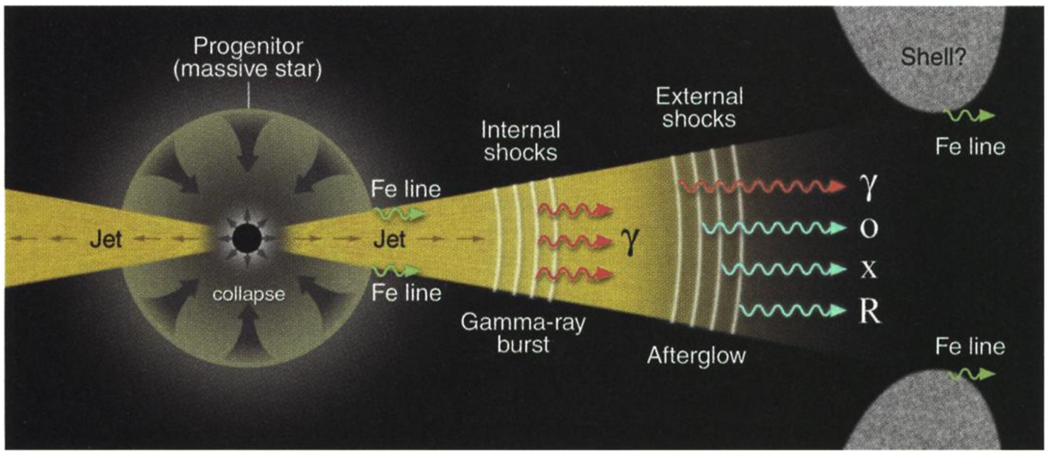

Fig. 3. Schematic GRB from a massive stellar progenitor, resulting in a relativistic jet that undergoes internal shocks, producing a burst of γ-rays and (as it decelerates through interaction with the external medium) an external shock afterglow, which leads successively to γ-rays, x-rays, optical, and radio. Iron lines may arise from x-ray illumination of a pre-ejected shell (e.g., supernova remnant) (*60*) or from continued x-ray irradiation of the outer stellar envelope (*67*).

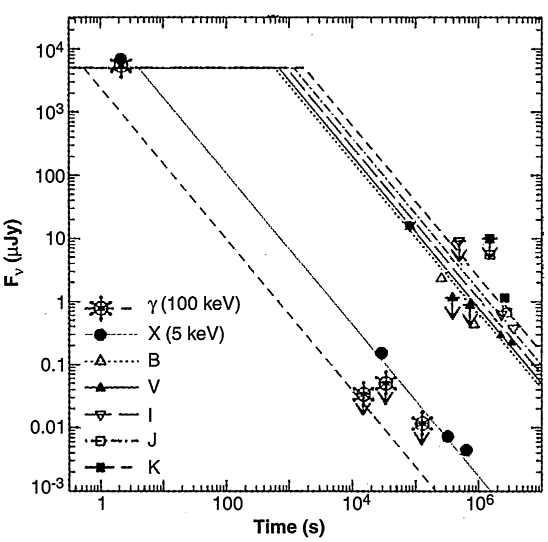

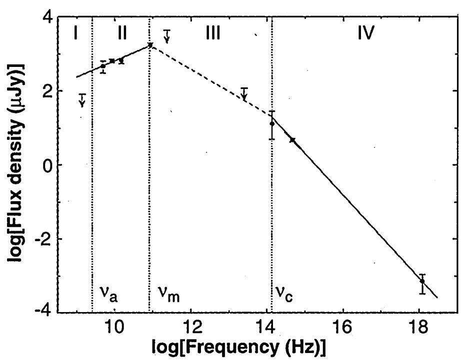

Fig. 4 (left). Comparison (*26*) of the observed light curves of the afterglow of GRB970228 at various wavelengths with the simple blast wave model predictions (*23*). **Fig. 5 (right).** Snapshot spectrum of GRB970508 at t = 12 days after the burst, compared to a standard afterglow synchrotron shock model fit (*29*).

velocities would take these binaries, in more than half of the cases, outside of the confines of the host galaxy before they merge and produce a burst. However, these calculations are uncertain because they are sensitive to a number of poorly known parameters (e.g., distribution of initial separations). On the other hand, theoretical estimates (*45*) suggest that NS-NS and NS-BH mergers will lead to shorter bursts ($\lesssim 5$ s), beyond the capabilities of BeppoSAX but expected to be detectable with the recently launched HETE-2 spacecraft (*54*) and the Swift multiwavelength GRB afterglow mission (*55*) now under construction.

For the long burst afterglows localized so far, the host galaxies show signs of ongoing star formation activity, necessary for the presence of young, massive progenitor stars. Such stars generally form in dense gaseous clouds, for which there is some independent evidence from the observation of 0.5- to 2-keV absorption in the x-ray afterglow spectra, attributed to metals in a high column density of gas in front of the burst (*56*). X-ray atomic edges and resonance absorption lines are expected to be detectable from the gas in the immediate environment of the GRB, and in particular from the remnants of a massive progenitor stellar system (*57–59*). Observations with the Chandra ACIS x-ray spectrographic camera and with BeppoSAX have provided evidence, with a moderate confidence level, for iron Kα line and edge features in at least two bursts (*60, 61*). The observed frequencies of the iron lines appear displaced from the laboratory frequency, as expected from the Doppler shift caused by the expansion of the universe, in agreement with the redshift measured in optical lines from the host galaxy.

One possible interpretation of the iron lines is that x-rays from the afterglow illuminate an iron-enriched supernova remnant situated outside the burst region, leading to iron recombination line emission (Fig. 3). This would require the supernova explosion to have occurred days or weeks before the burst, associated with the same progenitor (*60, 62, 63*). There is independent support that, at least in some bursts, a supernova may be involved (*64–66*). This may have contributed to an otherwise unexplained bump and reddening in the optical light curve after several weeks, and similar reddened bumps have been reported in at least two other bursts. The presence of iron line features would strongly suggest a massive stellar progenitor (*60*), but the details remain dependent on the model. Even without a pre-ejected supernova shell, a continued decaying x-ray emission from the GRB outflow impacting the outer stellar envelope (*63, 67*) may explain the iron lines.

The simple picture of an origin in star-forming regions, at least for the long ($t_b \gtrsim 5$ s) bursts, is complicated by the fact that the observed optical absorption is less than expected for the corresponding x-ray absorption. Also, standard afterglow model fits indicate an ambient gas density generally lower than that expected in star-forming clouds (*56*). However, these contradictions may be reconcilable, for example through dust sublimation by x-ray/UV radiation or the blowing out of a cavity by a progenitor wind.

Although it is unclear whether there is one or more than one class of GRB progenitors (e.g., corresponding to short and long bursts), there is a general consensus that they would all lead to the generic fireball shock scenario. Much of the current effort is dedicated to understanding the different progenitor scenarios and trying to determine how the progenitor and the burst environment can affect the observable burst and afterglow characteristics.

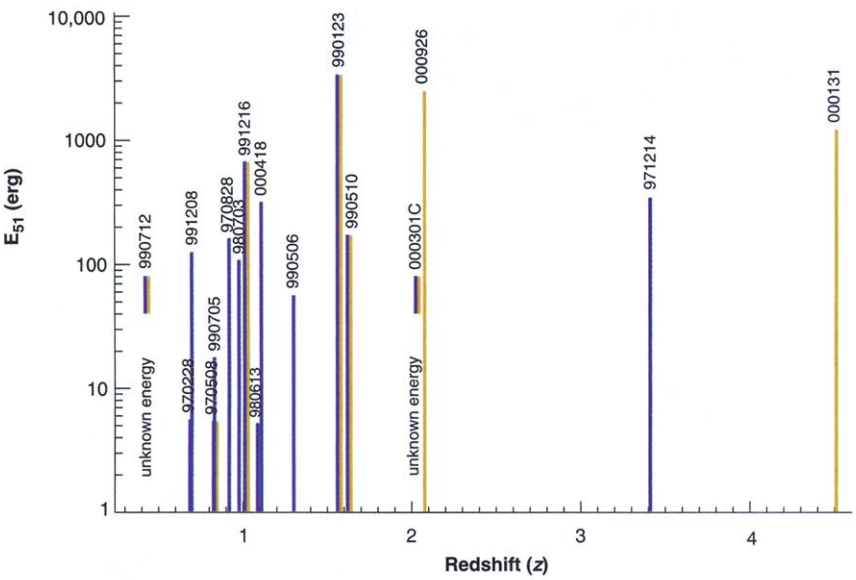

Fig. 6. The observed energy-redshift relation for 17 GRBs with optical spectroscopic redshifts as of 27 October 2000. Blue (orange) denotes that the redshift was found with emission (absorption) lines from the presumed host galaxy. The energy is derived from the γ-ray fluences reported and assumes that the GRB emitted energy isotropically. [Courtesy of J. S. Bloom and the Caltech GRB group]

Galactic Hosts and Cosmological Setting

For the long GRB afterglows localized so far, a host galaxy has been found in most cases (a growing number, more than 20 of 30 optically identified). The GRB host galaxies are typically of low mass and have the blue color and atomic spectral lines indicative of active star formation (*11*). The redshifts of the hosts, with one exception, are in the range $0.43 \lesssim z \lesssim 4.5$ (Fig. 6), that is, comparable to that of the most distant objects detected in the universe (about 10^{10} light years). The observed number of bursts per unit photon flux can be fitted by cosmological distribution models, with a somewhat better fit if one assumes that the burst rate scales proportionally to the observed star-formation rate as a function of redshift (*68–70*). The spread in the inferred luminosities (Fig. 6) is too broad to allow the use of GRBs as standard candles for the purpose of testing cosmological models (*71*). This spread in the inferred luminosities obtained under the assumption of isotropic emission may be reduced if most GRB outflows are jet-like, because in this case the measured flux is more intense when observed closer to the jet axis, as the result of an increased Doppler boost.

The bursts for which redshifts are known are bright enough to be detectable, in principle, out to much larger distances than those of the most luminous quasars or galaxies detected at present (*72*). Within the first minutes to hours after the burst, the optical light from afterglows is known to have a range of $m_v \sim 10$ to 15, far brighter than quasars, albeit for a short time. Thus, promptly localized GRBs could serve as beacons, shining through the pregalactic gas, that provide information about much earlier epochs in the history of the universe. The presence of iron or other x-ray lines provides an additional tool for measuring GRB distances, which may be valuable for investigating the small but puzzling fraction of bursts that have been detected only in x-rays but not optically, perhaps because of a high dust content in the host galaxy.

The newly launched HETE spacecraft (*54*) is expected to yield localizations for about 30 bursts per year, and as many as 200 to 300 per year are expected to be localized with the Swift spacecraft (*55*) due for launch in 2003. Swift will be equipped with γ-ray, x-ray, and optical detectors for on-board follow-up. It will be capable of relaying to the ground, within less than a minute from the burst trigger, burst coordinates of arc-second quality, allowing even mid-size ground-based telescopes to obtain prompt spectra and redshifts. This will permit much more detailed studies of the burst environment, the host galaxy, and the intergalactic medium between galaxies. The diffuse gas around a GRB is expected to produce time-variable optical/UV atomic absorption lines in the first minutes to hours after a burst (*73*), and additional hydrogen Lyman α absorption from intervening newly formed galaxies would be detectable as the GRB optical/UV continuum light shines through them (*74*). Although the starlight currently detected is thought to come mostly from later, already metal-enriched generations of star formation, GRBs arising from the earliest generation of stars may be detectable; if this occurs before galaxies have gravitationally assembled, it would provide a glimpse into the pregalactic phase of the universe.

Cosmic Rays, Neutrinos, and Gravitational Waves

There are other, as yet unconfirmed but potentially interesting, manifestations of GRBs. The same shocks that are thought to accelerate the electrons responsible for the nonthermal γ-rays in GRBs should also accelerate protons. Both the internal and the external reverse shocks are mildly relativistic, and are expected to lead to relativistic proton energy spectra of the form $dN_p/d\varepsilon_p \propto \gamma^{-p}$, where $p = 2$ to 2.5. The maximum proton energies achievable in GRB shocks are $E_p \sim 10^{20}$ eV, comparable to the highest energies measured with large arrays of cosmic ray detectors on the ground [e.g., (*75*)]. For this, the acceleration time must be shorter than both the radiation or adiabatic loss time and the escape time from the acceleration region. The resulting constraints on the magnetic field and the bulk Lorentz factor (*76*) are close to those required to obtain efficient γ-ray emission at $\sim$1 MeV. If the accelerated electrons that produce the γ-rays and the protons carry a similar fraction of the total energy, the GRB cosmic ray energy production rate at 10^{20} eV throughout the universe is on the order of 10^{44} erg Mpc^{-3} year^{-1}, comparable to the observationally required rate from γ-ray observations and from the observed diffuse cosmic ray flux (*76, 77*). These numbers depend to some extent on uncertainties in the burst total energy and beaming fraction, as well as on the poorly constrained burst rate evolution with redshift.

The accelerated protons can interact with the fireball photons, leading to charged pions, muons, and neutrinos. This reaction peaks at the energy threshold for the photo-meson Δ resonance. For internal shocks producing observed 1-MeV photons, this implies $\gtrsim 10^{16}$ eV protons, and neutrinos with $\sim$5% of that energy, $\varepsilon_\nu \gtrsim 10^{14}$ eV. Above this threshold, the fraction of the proton energy lost to pions is $\sim$20% for typical fireball parameters, and the typical spectrum of neutrino energy per decade is flat, $\varepsilon_\nu^2 \Phi_\nu \sim$ constant (*78*). Synchrotron and adiabatic losses limit the muon lifetimes (*79*), leading to a suppression of the neutrino flux above $\varepsilon_\nu \sim 10^{16}$ eV. Another copious source of target photons in the UV is the afterglow reverse shock, for which the resonance condition requires higher energy protons leading to neutrinos of 10^{17} to 10^{19} eV (*80*). These neutrino fluxes are expected to be detectable above the atmospheric neutrino background with the planned cubic kilometer ICECUBE Cherenkov detector (*81*).

Another mechanism for neutrino production in GRB is inelastic nuclear collisions. Whereas photo-pion interactions lead to higher energy neutrinos and provide a direct probe of the shock proton acceleration as well as of the photon density, inelastic proton-neutron collisions may occur even in the absence of shocks, leading to charged pions and neutrinos (*82*) with lower energies than those from photo-pion interactions. Provided the fireball has a substantial neutron/proton ratio, as expected in most GRB progenitors, the inelastic process is most intense when the nuclear scattering time scale becomes comparable to the expansion time scale, at which point the relative velocities of the nuclei become large enough to collide inelastically, resulting in charged pions and neutrinos (*83*). Inelastic collisions can also occur in fireball outflows with transverse inhomogeneities in the bulk Lorentz factor (*84*). The typical neutrino energies are in the 1- to 10-GeV range, which could be detectable for a sufficiently close phototube spacing in cubic kilometer detectors, in coincidence with observed GRBs.

The photo-pion and inelastic collisions responsible for the ultrahigh-energy neutrinos will also lead to neutral pions and electron-positron pair cascades, resulting in photons with GeV to TeV energies. A tentative $\gtrsim$0.1 TeV detection of a GRB has been reported with the water Cherenkov detector Milagrito (*85*). Other large atmospheric Cherenkov detectors, as well as planned space-based large-area solid-state detectors such as GLAST (*86*), will be able to measure photons in this energy range, which would be coincident with the neutrino pulses and the usual MeV γ-ray event. Their detection would provide important constraints on the emission mechanism of GRBs.

GRBs are also expected to be sources of gravitational waves. A time-integrated luminosity on the order of a solar rest mass ($\sim 10^{54}$ erg) is predicted from merging NS-NS and NS-BH models, whereas the luminosity from collapsar models is less certain but is estimated to be lower. Calculations (*87*) of the rates of gravitational wave events detectable by the Laser Interferometric Gravitational Wave Observatory (LIGO, currently under construction) from compact binary mergers, in coincidence with GRBs, has been estimated at a few per year for the initial LIGO, and up to 10 to 15 per year after the upgrades planned 2 to 4 years after first operations. The observation of such gravitational waves would be facilitated if the mergers involve observed GRB sources; conversely, it may be possible to strengthen the case for (or against) NS-NS or NS-BH progenitors of GRBs if gravitational waves were detected (or not) in coincidence with some bursts.

In conclusion, our understanding of GRBs has come a long way since their discovery almost 30 years ago, but these enigmatic sources continue to offer major puzzles and challenges. Several new space missions and ground experiments dedicated to GRB studies will come online in the near future, which should answer many of the questions discussed here. If past experience is any guide, they will also undoubtedly come up with new surprises and challenges.

References and Notes

1. G. Fishman, C. Meegan, *Annu. Rev. Astron. Astrophys.* **33**, 415 (1995).
2. D. Band *et al.*, *Astrophys. J.* **413**, 281 (1993).
3. K. Hurley *et al.*, *Nature* **372**, 652 (1994).
4. C. Kouveliotou *et al.*, *Astrophys. J.* **413**, L101 (1993).
5. E. Fenimore, E. Ramirez-Ruiz, B. Wu, *Astrophys. J.* **518**, L73 (1999).
6. E. Costa *et al.*, *Nature* **387**, 783 (1997).
7. J. van Paradijs *et al.*, *Nature* **386**, 686 (1997).
8. M. Metzger *et al.*, *Nature* **387**, 878 (1997).
9. S. Kulkarni *et al.*, *Proc. 5th Huntsville GRB Symposium*, in press (available at http://xxx.lanl.gov/abs/astro-ph/0002168).
10. D. Frail *et al.*, *Proc. 5th Huntsville GRB Symposium*, in press (available at http://xxx.lanl.gov/abs/astro-ph/9912171).
11. J. Bloom, R. Kulkarni, G. Djorgovski, in preparation (available at http://xxx.lanl.gov/abs/astro-ph/0010176).
12. B. Paczyński, *Astrophys. J.* **308**, L43 (1986).
13. J. Goodman, J., *Astrophys. J.* **308**, L47 (1986).
14. A. Shemi, T. Piran, *Astrophys. J.* **365**, L55 (1990).
15. M. J. Rees, P. Mészáros, *Mon. Not. R. Astron. Soc.* **258**, P41 (1992).
16. P. Mészáros, M. J. Rees, *Astrophys. J.* **405**, 278 (1993).
17. M. J. Rees, P. Mészáros, *Astrophys. J.* **430**, L93 (1994).
18. C. Dermer, K. Mitman, *Astrophys. J.* **513**, L5 (1999).
19. R. Blandford, D. Eichler, *Phys. Rep.* **154**, 1 (1987).
20. P. Mészáros, M. J. Rees, H. Papathanassiou, *Astrophys. J.* **432**, 181 (1994).
21. B. Paczyński, J. Rhoads, *Astrophys. J.* **418**, L5 (1993).
22. J. Katz, *Astrophys. J.* **432**, L107 (1994).
23. P. Mészáros, M. J. Rees, *Astrophys. J.* **476**, 232 (1997).
24. M. Vietri, *Astrophys. J.* **478**, L9 (1997).
25. M. Tavani, *Astrophys. J.* **483**, L87 (1997).
26. R. Wijers, M. J. Rees, P. Mészáros, *Mon. Not. R. Astron. Soc.* **288**, L51 (1997).
27. D. Reichart, *Astrophys. J.* **485**, L57 (1997).
28. R. Sari, T. Piran, R. Narayan, *Astrophys. J.* **497**, L17 (1998).
29. R. Wijers, T. Galama, *Astrophys. J.* **523**, 177 (1999).
30. T. Piran, *Phys. Rep.* **314**, 575 (1999).
31. J. van Paradijs, C. Kouveliotou, R. Wijers, *Annu. Rev. Astron. Astrophys.*, in press (available at http://astro.AnnualReviews.org/current.shtml).
32. J. Goodman, *New Astron.* **2**, 449 (1997).
33. E. Waxman, D. Frail, S. Kulkarni, *Astrophys. J.* **497**, 288 (1998).
34. S. Kulkarni *et al.*, *Nature* **398**, 389 (1999).
35. A. Fruchter *et al.*, in preparation (available at http://xxx.lanl.gov/abs/astro-ph/9902236).
36. A. J. Castro-Tirado *et al.*, *Science* **283**, 2069 (1999).
37. R. Sari, T. Piran, J. Halpern, *Astrophys. J.* **519**, L17 (1999).
38. K. Akerlof *et al.*, *Nature* **398**, 400 (1999).
39. R. Sari, T. Piran, *Astrophys. J.* **517**, L109 (1999).

40. J. Norris, G. Marani, J. Bonnell, *Astrophys. J.* **534**, 248 (2000).
41. E. Fenimore, E. Ramirez-Ruiz, in preparation (available at http://xxx.lanl.gov/abs/astro-ph/0004176).
42. D. Reichart *et al.*, in preparation (available at http://xxx.lanl.gov/abs/astro-ph/0004302).
43. S. Woosley, *Astrophys. J.* **405**, 273 (1993).
44. B. Paczyński, *Astrophys. J.* **494**, L45 (1998).
45. C. Fryer, S. Woosley, D. Hartmann, *Astrophys. J.* **526**, 152 (1999).
46. Hypernovae (*44*) are massive rotating stars whose core collapse is expected to lead to a BH accreting from a debris torus resulting in a GRB, as well as the ejection of a supernova remnant shell of energy above that of usual supernovae. Collapsars (*45*) are massive stars, which in the course of merging with a compact companion undergo core collapse leading to a BH, some of which result in a GRB, leaving a supernova-like remnant. Magnetars are ultrahigh magnetic field ($B \gtrsim 10^{15}$ G), fast-rotating (initially $\gtrsim$millisecond period) neutron stars, essentially super-pulsars (*50, 51*) resulting in a GRB; they would be created by the collapse of a massive rotating star leaving a supernova remnant. A supranova (*62*) is a massive star whose initial core collapse would lead to a neutron star and an ejected supernova remnant; this precedes by days to weeks a second collapse of the neutron star into a BH, which leads to a GRB. NS-NS and NS-BH mergers (*12*) also lead to a BH accreting from a debris torus, which wold be expected to lead to a GRB of comparable energy to those from massive stars (*49*); supernova remnants from the formation of the initial NS or BH would have occurred and dissipated $\gtrsim 10^7$ to 10^8 years before the GRB. In all of these cases, strong magnetic fields and $e^{\pm}$, γ from neutrino-antineutrino annihilation are expected to drive a jet-like relativistic outflow that leads to the standard fireball shock production of GRB and afterglows (*44, 45, 48*). In the massive progenitor cases, this would occur after the jet funnels through the stellar envelope, probably leading to a highly collimated jet, whereas in the NS-NS and NS-BH mergers the lack of an envelope might lead to substantially less collimation.
47. D. Eichler, M. Livio, T. Piran, D. N. Schramm, *Nature* **340**, 126 (1989).
48. P. Mészáros, M. J. Rees, *Astrophys. J.* **482**, L29 (1997).
49. ———, R. Wijers, *New Astron.* **4**, 313 (1999).
50. V. V. Usov, *Mon. Not. R. Astron. Soc.* **267**, 1035 (1994).
51. C. Thompson, *Mon. Not. R. Astron. Soc.* **270**, 480 (1994).
52. H. C. Spruit, *Astron. Astrophys.* **341**, L1 (1999).
53. R. D. Blandford, J. P. Ostriker, P. Mészáros, in preparation.
54. High Energy Transient Explorer (http://space.mit.edu/HETE).
55. Swift (http://swift.gsfc.nasa.gov).
56. T. Galama, R. Wijers, in preparation (available at http://xxx.lanl.gov/abs/astro-ph/0009367).
57. P. Mészáros, M. J. Rees, *Mon. Not. R. Astron. Soc.* **299**, L10 (1998).
58. C. Weth, P. Mészáros, T. Kallman, M. J. Rees, *Astrophys. J.* **534**, 581 (2000).
59. M. Böttcher, C. L. Fryer, in preparation (available at http://xxx.lanl.gov/abs/astro-ph/0006076).
60. L. Piro *et al.*, *Science* **290**, 955 (2000).
61. L. Amati *et al.*, *Science* **290**, 953 (2000).
62. M. Vietri, G. Perola, L. Piro, L. Stella, *Mon. Not. R. Astron. Soc.* **308**, L29 (2000).
63. In the supranova scenario (*60*), the interaction of the GRB afterglow with the supernova shell ejected weeks earlier and located about a light day from the burst is envisaged to give rise to Fe recombination lines; this requires in excess of 0.1 to 1 solar masses of Fe in the shell. In a decaying magnetar model (*67*), a long-lived ($\gtrsim$1 day) magnetar or accreting BH with a continuing but decaying jet interacts with the expanding stellar envelope to produce Fe recombination lines, requiring only a normal Fe abundance.
64. T. Galama *et al.*, *Nature* **395**, 670 (1998).
65. J. van Paradijs, *Science* **286**, 693 (1999).
66. J. C. Wheeler, in *Supernovae and Gamma Ray Bursts*, M. Livio, K. Sahu, N. Panagia, Eds. (Cambridge Univ. Press, Cambridge, in press) (available at http://xxx.lanl.gov/abs/9909096).
67. M. J. Rees, P. Mészáros, *Astrophys. J.*, in press (available at http://xxx.lanl.gov/abs/astro-ph/0010258).
68. R. Wijers, J. Bloom, J. Bagla, P. Natarajan, *Mon. Not. R. Astron. Soc.* **294**, L13 (1998).
69. T. Totani, *Astrophys. J.* **511**, 41 (1999).
70. A. Blain, P. Natarajan, *Mon. Not. R. Astron. Soc.* **312**, L35 (2000).
71. S. Mao, H. J. Mo, *Astron. Astrophys.* **339**, L1 (1998).
72. D. Q. Lamb, D. Reichart, *Astrophys. J.* **536**, L1 (2000).
73. R. Perna, A. Loeb, *Astrophys. J.* **508**, L135 (1998).
74. A. Loeb, R. Barkana, *Annu. Rev. Astron. Astrophys.*, in press (available at http://xxx.lanl.gov/abs/astro-ph/0010467).
75. N. Hayashida *et al.*, *Astrophys. J.* **522**, 225 (1999).
76. E. Waxman, *Phys. Rev. Lett.* **75**, 386 (1995).
77. C. Dermer, in preparation (available at http://xxx.lanl.gov/abs/astro-ph/0005440).
78. E. Waxman, J. N. Bahcall, *Phys. Rev. Lett.* **78**, 2292 (1997).
79. J. Rachen, P. Mészáros, *Phys. Rev. D* **58**, 123005 (1998).
80. E. Waxman, J. N. Bahcall, *Phys. Rev. D* **59**, 023002 (1999).
81. F. Halzen, *17th International Conference on Weak Interactions and Neutrinos* (available at http://xxx.lanl.gov/abs/astro-ph/9904216).
82. E. V. Derishev, V. V. Kocharovsky, Vl. V. Kocharovsky, *Astrophys. J.* **521**, 640 (1999).
83. J. N. Bahcall, P. Mészáros, *Phys. Rev. Lett.* **85**, 1362 (2000).
84. P. Mészáros, M. J. Rees, *Astrophys. J.*, in press (available at http://xxx.lanl.gov/abs/astro-ph/0007102).
85. R. Atkins *et al.*, *Astrophys. J.* **533**, L119 (2000).
86. N. Gehrels, P. Michelson, *Astropart. Phys.* **11**, 277 (1999).
87. L. S. Finn, S. Mohanty, J. Romano, *Phys. Rev. D* **60**, 121101 (1999).

88. Supported by NASA grants NAG5-9192 and NAG5-9153 and by NSF grant PHY94-07194.

REVIEW

Magnetohydrodynamic Production of Relativistic Jets

David L. Meier,[1]* Shinji Koide,[2] Yutaka Uchida[3]

A number of astronomical systems have been discovered that generate collimated flows of plasma with velocities close to the speed of light. In all cases, the central object is probably a neutron star or black hole and is either accreting material from other stars or is in the initial violent stages of formation. Supercomputer simulations of the production of relativistic jets have been based on a magnetohydrodynamic model, in which differential rotation in the system creates a magnetic coil that simultaneously expels and pinches some of the infalling material. The model may explain the basic features of observed jets, including their speed and amount of collimation, and some of the details in the behavior and statistics of different jet-producing sources.

A jet is a tightly collimated stream of fluid, gas, or plasma. It typically carries kinetic and internal energy and linear momentum, and if it is set spinning about its direction of motion by some means, it can carry angular momentum as well. A relativistic jet is one whose speed approaches the universally constant speed of light c = 299,792.5 km s^{-1}. At such velocities, Einstein's theory of relativity becomes important. The kinetic energy of motion (and possibly the internal thermal and magnetic energy as well) adds mass to the jet, equal to E_{kinetic}/c^2, making it more difficult to accelerate. Also, as seen by viewers at rest, time slows down in the moving jet material, and any light or radio emission from the jet tends to be radiated in the direction of flow, not isotropically, as would be the case if the flow velocity were subrelativistic. Because c is a maximum speed limit and because conditions become more extreme as it is approached, the Lorentz factor

$$\Gamma = \left(1 - \frac{v^2}{c^2}\right)^{-1/2} \tag{1}$$

is often used to characterize the speed, rather than the velocity v. For example, $\Gamma = 10$ describes a flow at 99.5% of c, with each particle in the jet having a mass 10 times as much as it has when it is at rest.

For analyzing observations of relativistic jets, the Doppler factor

$$D = \left[\Gamma\left(1 - \frac{v}{c}\cos\theta\right)\right]^{-1} \tag{2}$$

is an equally important parameter; θ is the angle between the jet flow direction and the observer's line of sight. For low-speed jets with $v \ll c$, this reduces to the familiar nonrelativistic Doppler factor $D \approx 1 + (v/c)\cos\theta$ that is responsible, for example, for the slight frequen-

[1]Jet Propulsion Laboratory, California Institute of Technology, Pasadena, CA 91109, USA. [2]Faculty of Engineering, Toyama University, Gofuku 3190, Toyama 930-8555, Japan. [3]Physics Department, Science University of Tokyo, Shinjuku-ku, Tokyo 162, Japan.

*To whom correspondence should be addressed. E-mail: David.L.Meier@jpl.nasa.gov